



Torsional strengthening of thin-walled tubular reinforced concrete structures using NSM-CFRP laminates: Experimental work

Chandan C. Gowda, Joaquim A. O. Barros

University of Minho, ISE, Guimarães, Portugal

Maurizio Guadagnini

The University of Sheffield, Sheffield, U.K

Contacting author: chandu627@gmail.com

Abstract

Torsional strengthening of thin walled tubular reinforced concrete elements, such as bridge box girders and spandrel beams, has received only limited attention, and investigations generally focus on the use of conventional strengthening methods such as span shortening, steel encasing, member enlargement, shotcrete etc. However, research on the use of innovative fibre reinforced polymers (FRP) as near surface mounted (NSM) reinforcement for torsional strengthening is still very limited and more work should be undertaken to examine the full potential of the NSM technique over more traditional solutions. The current paper assesses experimentally, four different strengthening configurations using NSM technique applied on three faces of two beams using straight CFRP laminates, and on four faces of two beams using special L-CFRP laminates.

The results show that the proposed strengthening configurations can effectively control crack propagation and increase the torsional moment carrying capacity of the RC element, thus resulting in increased performance and durability.

Keywords: Torsional strengthening, near surface mounted technique, box type structures, CFRP laminates.

1. Introduction

The growing increase of road and rail traffic, upgrades in standard codes, deficient construction, corrosion of steel and improper maintenance are causing the necessity of improving the service life of deficient structural elements, including reinforced concrete (RC) bridges. Since new construction is expensive in comparison with the rehabilitation of existing structures, there is a necessity to develop cost-effective, sustainable, rapid and easy-to-apply strengthening solutions to ensure adequate service performance and extend the service life of

existing structures. Most often, existing rehabilitation solutions involve the use of traditional construction materials such as concrete and steel, but more recently advanced materials such as fibre reinforced polymers (FRP's) and adhesives have been introduced. This paper investigates the application of near surface mounted (NSM) FRP reinforcement to strengthen torsional deficient structures like bridges, spandrel beams, circular staircases and other structural elements subjected to torsion.

Torsion is an area where limited investigation is available in terms of both experimental work and numerical analysis. However, a few studies on

torsional strengthening using externally bonded (EBR) FRP have been carried out and focus on investigating the behaviour of box type structures [1] and solid sectioned beams with anchored and extended U-jacket FRP strips [2]. One of the earliest applications of EBR FRP in torsional strengthening using glass FRP (GFRP) has been reported in [3], where the strengthening faces, fibre orientation, number of plies and influence of anchors were investigated. [4] and [5] proposed analytical models to predict the torsional behaviour of concrete structures retrofitted with FRP materials. In [6], FRP fabrics were used for the strengthening of RC T-beams submitted to combined shear and torsion.

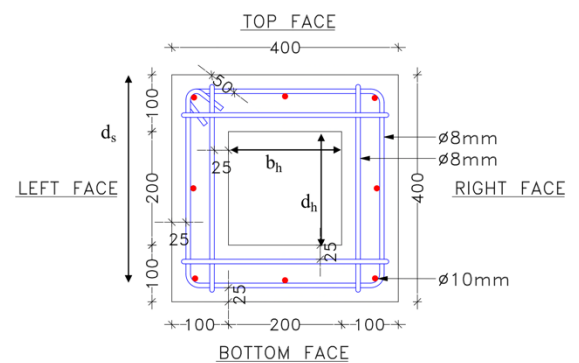
Recently, two investigations on torsional strengthening of solid sectioned beams using NSM technique have been carried out [7], [8]. In [7] eight beams were strengthened with CFRP laminates bonded to the concrete substrate with epoxy and cement based adhesives and it was concluded that the cement based adhesives are less efficient in increasing the torsional capacity. However, cement based adhesives are preferable in situations like fire, where epoxy adhesives have poor performance. In [8], eight beams were strengthened with CFRP ropes and straight laminates bonded with epoxy and cement adhesive. Based on the results obtained in this study, CFRP ropes were found to perform much better than the straight laminates, regardless the considered adhesive.

2. Experimental work

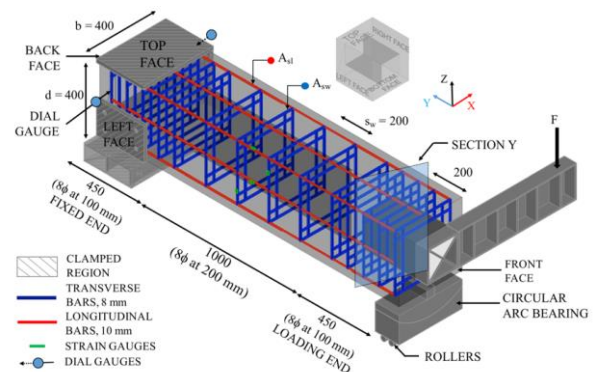
The experimental work reported in the current paper involves testing five beams in torsion, with one reference beam and four strengthened beams. Two series of strengthened elements are examined: (i) specimens strengthened on three faces using straight CFRP laminates and (ii) specimens strengthened with bespoke manufactured L-CFRP laminates. Both series comprise two beams, each one with different strengthening ratio, categorized as minimum (lower) and maximum (higher) strengthening ratio.

2.1 Geometry and material characterization

The cross-sectional and longitudinal details of the beam specimens are shown in Figure 1, with an outer cross section of 400×400 mm and an inner hollow section of 200×200 mm. Each beam is 1900 mm in length, with eight 10 mm diameter bars distributed in the corners and the middle of each side as longitudinal steel reinforcement, while the stirrups comprise 8 mm diameter with four legs. A clear cover of 25 mm is provided to both the exterior and interior faces. The transverse reinforcement is spaced at 200 mm in the central zone of 1000 mm (study region) and at 100 mm along the 450 mm long end zones (over-reinforced region). The spacing is decreased in the end regions to minimize the damage due to the loading and clamping conditions.



(a)



(b)

Figure 1 Beam geometry (a) Cross-section and (b) Longitudinal details (all dimensions are in mm)

Strain gauges are placed as close as possible to the central section of the beam (950 mm) and are

attached to both steel and CFRP reinforcements. Two strain gauges are attached to the longitudinal reinforcement and two strain gauges to the steel and CFRP laminate transverse reinforcement (Figure 1). The equivalent reinforcement ratios ($r_{l,eq}$ and $r_{w,eq}$) of the strengthened beams are calculated using equations (1) and (2). The corresponding values and the spacing of laminates in longitudinal (s_{fl}) and transverse (s_{fw}) directions are presented in where A_{sl} , b and d_s are, respectively, the cross sectional area, breadth and the internal arm of the existing longitudinal steel bars; A_f and d_f are the cross sectional area and the lever arm of the internal longitudinal CFRP; E_s and E_f are the modulus of elasticity of the steel and CFRP; b_w is the width of the web (100 mm); b_h and d_h are the breadth and depth of the hollow section; A_{sw} and s_w are the cross sectional area and the spacing of the transverse reinforcement (Figure 1b).

Table 1.

$$r_{l,eq} = \frac{A_{sl}}{(bd_s - b_h d_h)} + \left[\frac{A_f E_f}{E_s} \frac{1}{(bd_f - b_h d_h)} \right] \quad (1)$$

$$r_{w,eq} = \frac{A_{sw}}{(b_w s_w)} + \left[\frac{A_f E_f}{E_s} \frac{1}{(bs_f)} \right] \quad (2)$$

where A_{sl} , b and d_s are, respectively, the cross sectional area, breadth and the internal arm of the existing longitudinal steel bars; A_f and d_f are the cross sectional area and the lever arm of the internal longitudinal CFRP; E_s and E_f are the modulus of elasticity of the steel and CFRP; b_w is the width of the web (100 mm); b_h and d_h are the breadth and depth of the hollow section; A_{sw} and s_w are the cross sectional area and the spacing of the transverse reinforcement (Figure 1b).

Table 1. Longitudinal and transverse reinforcements in strengthened beams

Beam Description	$\rho_{l,eq}$	$r_{w,eq}$	s_{fl} (mm)	s_{fw} (mm)
S2_L2S5	0.64	0.55	134	65
S2_L4S10	0.71	0.61	80	40
S3L_L2S5	0.67	0.57	134	200
S3L_L4S10	0.76	0.64	80	200

The material properties of concrete, steel and CFRP laminates according to the tests performed in the laboratory are presented in Table 2. Compression tests are carried out on concrete cylinders of 150 mm diameter at 28 days according to the standard [9]. Three cylinders were tested to determine the average compressive strength (f_{cm}) and modulus of elasticity (E_{cm}). Tensile tests are performed on 8 mm and 10 mm diameter bars, with five samples each using the standards [10] and [11] to determine the tensile strength (f_t) and modulus of elasticity (E_s). The strengthening is performed using CFRP laminates of 10 mm × 1.4 mm and epoxy resin 220 from S&P manufacturer. Three specimens in each batch (see Table 2) are tested to determine the average tensile strength and modulus of elasticity of CFRP laminates according to the standard [12]. Beam S2_L2S5 and S2_L4S10 are strengthened with laminates from batch 2 both in the longitudinal and transverse direction, whereas beams S3L_L2S5 and S3L_L4S10 are strengthened with laminates from batch 3 in the longitudinal direction and from batch 4 (L-laminates) in the transverse direction.

Table 2 Properties of concrete, steel and FRP

Material	Compressive or tensile strength, MPa [Co.V.]	Modulus of elasticity, GPa [Co.V.]
Concrete	31.8 (3.0%)	34.5 (4.0%)
Steel (8 mm bar)	567 (7.5%)	196 (0.4%)
Steel (10 mm bar)	450 (2.69%)	206 (2.7%)
CFRP (batch 2)	1982 (3.0%)	200 (1.0%)

CFRP (batch 3)	1879 (0.5%)	199 (0.1%)
CFRP (batch 4, L-laminates)*	2276 (0.6%)	196 (0.1%)

*the values provided corresponds to tests of laminates before transforming them to L-type.

2.2 Strengthening configurations

A finite element (FE) study was carried out to assist with the design of the experimental test setup and testing protocols. The numerical model was calibrated against an available set of experimental data and several strengthening configurations were investigated [13]. Based on the outcome of this study, three strengthening solutions were proposed and explored. Series one involves strengthening on all four faces of the beams (four beams) and the results of these experimental tests are described in detail in [14]. Series two involves strengthening only on three faces, and series three uses strengthening on four faces with L type CFRP laminates. The results of these last two series are discussed in this paper.

2.2.1 Series two

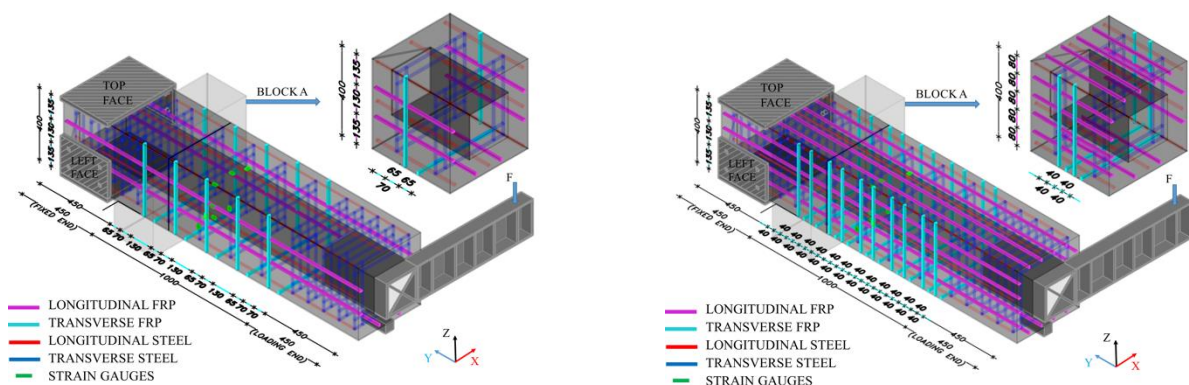
Two beams are strengthened in this series with minimum and maximum strengthening ratios as presented in where A_{sl} , b and d_s are, respectively, the cross sectional area, breadth and

the internal arm of the existing longitudinal steel bars; A_f and d_f are the cross sectional area and the lever arm of the internal longitudinal CFRP; E_s and E_f are the modulus of elasticity of the steel and CFRP; b_w is the width of the web (100 mm); b_h and d_h are the breadth and depth of the hollow section; A_{sw} and s_w are the cross sectional area and the spacing of the transverse reinforcement (Figure 1b).

Table 1. In real-life scenarios it is usually difficult or almost impossible to strengthen all four faces of the beams due to presence of either slabs or beams or other structural and non-structural elements. As a result, series 2, which uses strengthening on only three faces, was examined. The isometric section of the strengthening schemes is shown in Figure 2(a) and (b).

2.2.2 Series three

This series consists of two strengthened beams with minimum and maximum strengthening ratios as adopted in series one [14]. However, L-CFRP laminates were used instead of straight CFRP laminates adopted in series one and two. Figure 2(c) and 2(d) show the strengthening configuration of series three.



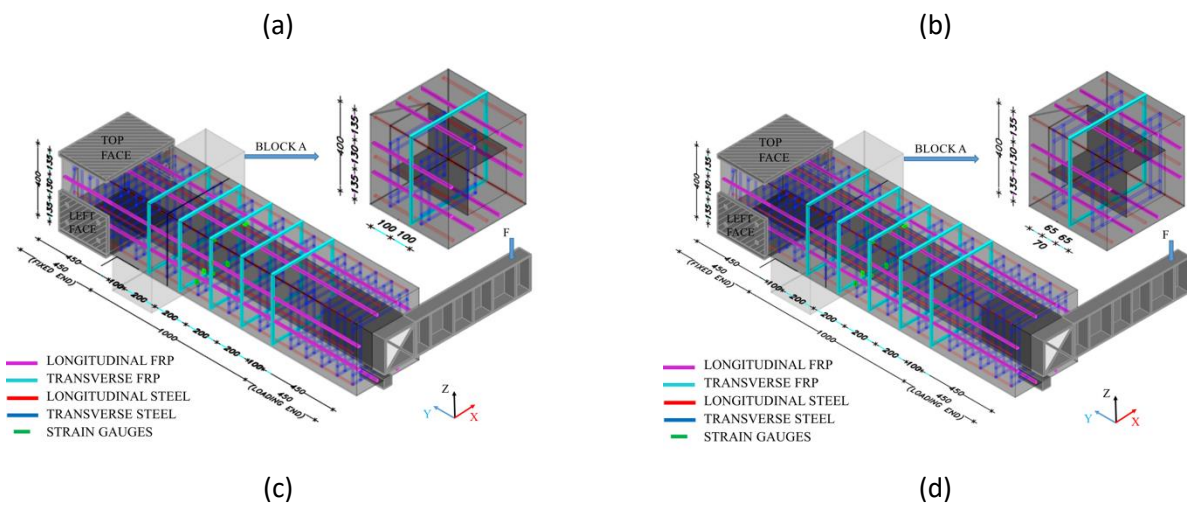


Figure 2 Strengthening configurations of series two and three (a) S2_L2S5, (b) S2_L4S10, (c) S3L_L2S5 and (d) S3L_L4S10 (all dimensions are in mm)

2.3 Test setup

The experimental test setup to perform the torsional tests on beams is as shown in Figure 3. It consists of two ends i.e., fixed end and loading end. The load is applied through a steel section, which is connected to the load cell in one end and the other end is inserted inside the hollow section of the beam up to a length of 300 mm. Multiple hinges are placed above and below this steel loading section to avoid any eccentric or parasitic forces during testing. In order to ensure that no failure takes place in the over-reinforced loading end, 52 mm wide steel jackets, inter-connected through bolts are placed at two locations, separated by a distance of 400 mm (Figure 3). A circular arc-bearing (CAB) is placed below the pinned support on which the beam rests (loading end), to allow free rotation of the beam with a circular arc radius of 350 mm from the centre of the beam. Rollers are placed below the CAB to allow axial deformation of the beam during tests.

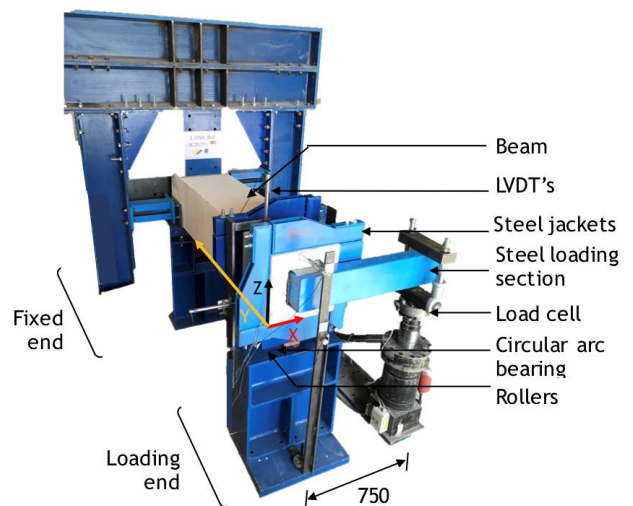


Figure 3 Test setup for the experimental work

The fixed end consists of steel sections in all the four directions (mainly I-sectioned frames) to ensure as much as possible the complete fixity of the beam. A hydraulic jack is also placed at the base of the beam to adjust its location before testing. Multiple sensors like LVDT's, dial gauges and inclinometers are used to measure displacement and torsional angle of rotation for data acquisition and analysis. Four LVDT's are placed in between the steel jackets (on each face) to measure the rotational angle and also an inclinometer is placed inside the hollow section for the same purpose. Two LVDT's each are placed along the front and rear faces of the beam to measure the beam's axial deformation. Dial

gauges are located on the central right and left faces of the beam in the fixed end to measure any possible transversal movement of the beam in this region. The torsional tests are performed under displacement control at a rate of 1.2 mm/min.

3. Results and discussion

The torsional moment vs. torsional angle of rotation of the beams of series two and three, including the reference beam, is shown in Figure 4 and the relevant results are presented in Table 3. In terms of ultimate torsional moment, the beams with the minimum strengthening ratio (S2_L2S5 and S3L_2S5) had an average increase of 18.7 kN·m, while the beams with the maximum strengthening ratio (S2_L4S10 and S3L_L4S10) had an average increase of 31.1 kN·m, corresponding to an increase that varied between 17.6% and 38.2%. Except beam S2_L2S5, the adopted strengthening configurations have provided an increase of the torsional angle of rotation at beam's failure, with the highest increase (74.8%) in beam S3L_L4S10, which represents an improvement in terms of ductility.

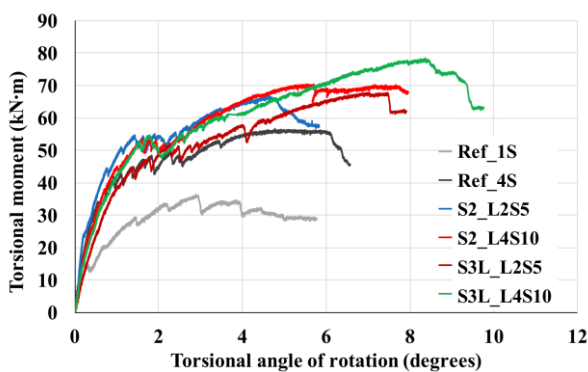


Figure 4 Torsional moment vs. torsional angle of rotation of series two and three

Table 3 Experimental results of series two and series three

Sl. No. [units]	Beam description	Max. torsional moment [kN·m]	Percentage increase [%]	Angle at maximum torsion [degrees]	Max. strain in steel [$\mu\epsilon$]	Max. strain in CFRP [$\mu\epsilon$]	Average crack spacing [mm]
1	Ref_4S	56.7	-	4.8	19825	-	200.3
2	S2_L2S5	66.6	17.6	4.6	20719	4319	169.2

The torsional behaviour of the strengthened beams can be split into three phases: (i) Linear phase: up to torsional cracking moment; (ii) crack propagation phase: where micro and macro cracks are formed, taking place between torsional cracking moment and yielding of the steel reinforcement. The steel and the CFRP reinforcements start resisting torsion only after torsional cracking moment ($m_{t,cr}$), which is clearly observed in the torsional moment vs. steel strain evolution, and in the torsional moment vs. CFRP strain evolution shown in Figure 5. Only beam S2_L4S10 and S3L_L2S5 strain evolution are presented due to lack of space. However, all other beams follow a similar pattern.

All the steel reinforcing bars in all the beams have yielded before the ultimate torsional moment of the corresponding beam is reached (as captured through strain gauges). Finally, (iii) yielding phase: where steel reinforcements are yielded and the increase of torsional moment is mainly ensured by CFRP laminates. The performance of the steel reinforcements can also be split into two parts, i.e., before and after torsional cracking moment. The steel reinforcements have almost null contribution up to $m_{t,cr}$ and a sudden jump is observed (Figure 5a) after cracking. Similarly, the performance of CFRP laminates can be categorized into three parts: (i) up to torsional cracking moment with the minimum contribution of the laminates; (ii) in the crack propagation phase with simultaneous participation of CFRP laminates and steel reinforcement, up to the yielding of the steel reinforcement; and (iii) phase where the CFRP laminates play a vital role in resisting the torsional moment until failure occurs.

3	S2_L4S10	70.3	23.9	5.7	21234	4545	139.9
4	S3L_L2S5	67.9	19.7	7.0	-	5979	119.7
5	S3L_L4S10	78.3	38.2	8.4	4852	4542	88.7

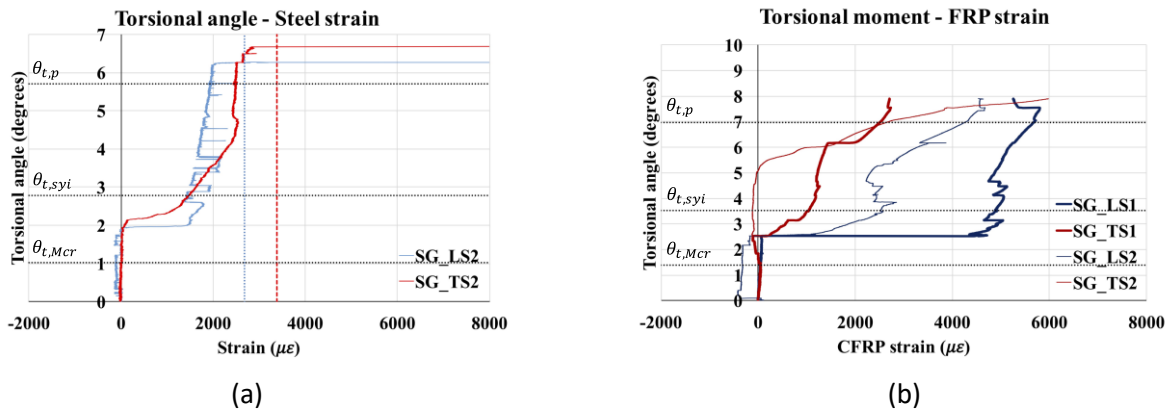


Figure 5 (a) S2_L4S10 Torsional angle vs. steel strain and (b) Torsional angle vs. FRP strains of beam S3L_L2S5

Figure 6 shows the images of beams at respective failure locations. Beam S2_L2S5 and S2_L4S10 failed by concrete crushing on the unstrengthened surface (top face) of the beams. However, beam S2_L4S10 failed prematurely by concrete crushing in between the steel jackets at the loading end (over-reinforced region) due to stress concentration from the steel loading section.

Series three beams with L-CFRP type laminate failed by CFRP rupture in the transition zone followed by concrete crushing. The failure of the CFRP laminates were confirmed by the post-test inspection, which were also confirmed by loud noise during testing and by video recordings. The zone along which CFRP laminate rupture was observed is indicated by a red box in Figure 6.



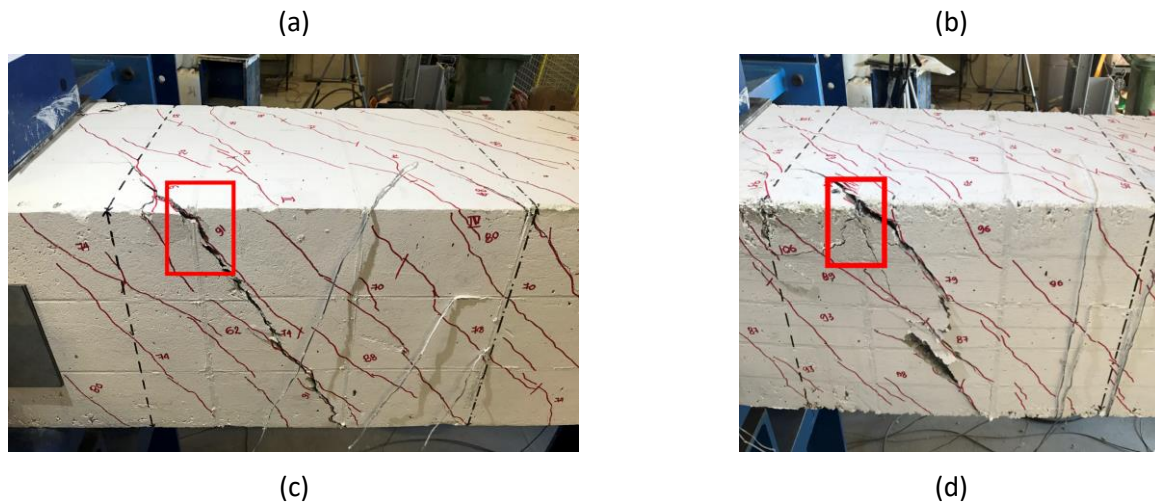


Figure 6 Failure images (a) S2_L2S5 (b) S2_L4S10 (c) S3L_L2S5 and S3L_L4S10

The CFRP laminates are successful in arresting the crack propagation, thereby reducing the crack spacing and increasing the torsional moment carrying capacity of the beam. All the strengthened beams have smaller crack spacing in comparison with the reference beam, varying between 15.5% and 55.7%, with the maximum reduction in beam S3L_L4S10. Failure due to bond (concrete/CFRP or CFRP/epoxy) or corner rupture (usually in case of torsion), which are common for externally bonded reinforcement (EBR), was not observed in any of the current strengthening configurations. Although the beams tested in series three and strengthened on all the four faces performed better, the beams with strengthening on only three faces (series two) have a very good overall behavioural response. Beams in series three had a better ductile behaviour due to strengthening on all four faces, even though it had higher spacing of the transverse CFRP laminates, sufficient enough to arrest the spiral crack growth.

4. Conclusions

Based on the results obtained from the current work, the following conclusions can be drawn:

- All the strengthened beams exhibited an improved torsional behaviour in terms of torsional moment capacity (17.6%-38.2%), corresponding torsional angle of rotation (19.5%-74.8%), smaller crack spacing (15.5%-55.7%) and controlled crack propagation;

- Almost all the steel reinforcing bars yielded before the maximum torsional capacity was reached. The CFRP laminates reached maximum strains of 5.67‰, which is 58% of their tensile rupture;
- Beams strengthened on three faces (series two) failed by concrete crushing on the unstrengthened surface and the L-laminate strengthened beams failed by CFRP-rupture in the transition zone followed by concrete crushing.

5. Acknowledgements

The author would like to thank the Marie Curie Initial Training Network “Endure” for the grant received and also the Portuguese Foundation for Science and Technology for the current FCT grant. The author would also like to extend the acknowledgements to the industries CASAIS and CiviTest for performing the experimental work. The authors acknowledge the support provided by the FCT for the project StreColesf, POCI-01-0145-FEDER-029485.

6. References

1. Hii AKY, Al-Mahaidi R. An experimental and numerical investigation on torsional strengthening of solid and box-section RC beams using CFRP laminates. *Compos Struct.* 2006;75(1–4):213–21.
2. Deifalla A, Awad A, Elgarhy M. Effectiveness of externally bonded CFRP

- strips for strengthening flanged beams under torsion: An experimental study. *Eng Struct* [Internet]. Elsevier Ltd; 2013;56:2065–75.
3. Panchacharam S, Belarbi A. Torsional Behavior of Reinforced Concrete Beams Strengthened with FRP Composites. In: *First FIB Congress on Concrete Structures in 21st Century*, Osaka, Japan, October 13-19, 2002. 2002. p. 1–11.
 4. Deifalla A, Ghobarah A. Simplified analysis for Torsionally Strengthened RC Beams Using FRP. In: *Proceedings of International Symposium on Bond Behaviour of FRP in Structures (BBFS 2005)*, Hong Kong, December 5-7, 2005. 2005.
 5. Chalioris CE. Analytical model for the torsional behaviour of reinforced concrete beams retrofitted with FRP materials. *Eng Struct*. 2007;29(12):3263–76.
 6. Deifalla A, Ghobarah A. Strengthening RC T-Beams Subjected to Combined Torsion and Shear Using FRP Fabrics : Experimental Study. *J Compos Constr* © ASCE / MAY/JUNE 2010. 2010;(June):301–12.
 7. Al-Bayati G, Al-Mahaidi R, Kalfat R. Torsional strengthening of reinforced concrete beams using different configurations of NSM FRP with epoxy resins and cement-based adhesives. *Compos Struct* [Internet]. 2017;168:569–81.
 8. Al-Bayati G, Al-Mahaidi R, Hashemi MJ, Kalfat R. Torsional strengthening of RC beams using NSM CFRP rope and innovative adhesives. *Compos Struct* [Internet]. Elsevier; 2018;187(December 2017):190–202.
 9. BS EN 12390-3 (2009). Testing hardened concrete. 2009.
 10. EN_10002-1 (1990). Metallic materials Tensile testing Part 1: method of test at ambient temperature. *Eur Comm Stand* [Internet]. 2001;
 11. ISO 6892-1. Metallic materials — Tensile testing — Part 1: Method of test at room temperature. *Metallic Materials*. 2009.
 12. ISO 527-5. Plastics — Determination of tensile properties - Part 5: Test conditions for unidirectional fibre-reinforced plastic composites [Internet]. International Organisation for Standardization (ISO), Geneva, Switzerland. 1997.
 13. Gowda CC, Barros JAO. Exploring NSM technique for torsional strengthening of tubular type RC structures. In: *11th fib International symposium in Civil Engineering*. University of Tokyo, Japan, Aug 29th-31st, 2016; 2016. p. 1–8.
 14. Gowda CC, Barros JAO, Gua. Experimental Investigation on Torsional Strengthening of Box RC structures using NSM FRP. In: *9th International conference on Fibre-reinforced polymer (FRP) composites*. 2018.